

1 **Non biogenic source is an important but**
2 **overlooked contributor to aerosol isoprene-**
3 **derived organosulfates during winter in**
4 **northern China**

5

6 Ting Yang¹, Yu Xu^{1,2*}, Yu-Chen Wang³, Yi-Jia Ma¹, Hong-Wei Xiao^{1,2}, Hao Xiao^{1,2},
7 Hua-Yun Xiao^{1,2}

8

9 ¹School of Agriculture and Biology, Shanghai Jiao Tong University, Shanghai 200240,
10 China

11 ²Shanghai Yangtze River Delta Eco-Environmental Change and Management
12 Observation and Research Station, Ministry of Science and Technology, Ministry of
13 Education, Shanghai 200240, China

14 ³Division of Environment and Sustainability, Hong Kong University of Science and
15 Technology, Hong Kong SAR 00000, China

16

17 *Corresponding authors

18 Yu Xu

19 E-mail: xuyu360@sjtu.edu.cn

20

21 **Abstract:** Previous measurement-model comparisons of atmospheric isoprene levels
22 showed a significant unidentified source of isoprene in some northern Chinese cities
23 during winter. Here, spatial variability in winter aerosol organosulfate (OS) formation
24 in typical southern (Guangzhou and Kunming) and northern (Xi'an and Taiyuan)
25 cities, China, was investigated to reveal the influence of potential non biogenic
26 contributor on aerosol OS pollution levels. Monoterpene-derived OSs were
27 significantly higher in southern cities than in northern cities, which was attributed to
28 temperature dependent emission of monoterpenes (i.e., higher temperatures in
29 southern cities drove more monoterpene emissions). However, isoprene-derived OSs
30 (OS_i) showed the opposite trend, with significantly higher levels in northern cities.
31 Principal component analysis combined with field simulation combustion experiments
32 suggested that biomass burning rather than gasoline, diesel, and coal combustion
33 contributed significantly to the abundance of OS_i in northern cities. The comparison
34 of anthropogenic OS molecular characteristics between particles released from
35 various combustion sources and ambient aerosol particles suggested that stronger
36 biomass and fossil fuel combustion activities in northern cities promoted the
37 formation of considerable anthropogenic OSs. Overall, this study provides direct
38 molecular evidence for the first time that non biogenic sources can significantly
39 contribute to the formation of OS_i in China during winter.

40

41 **Keywords:** Aerosol organosulfates, Biogenic precursors, Anthropogenic precursors,
42 Spatial variation, Influencing factors, **Biomass burning**

43 **1. Introduction**

44 Organosulfates (OSs) with a sulfate ester functional group typically contribute 3–
45 30% of the organic aerosol mass in atmospheric fine particles (PM_{2.5}) (Luk'Acs et al.
46 2009). Moreover, OSs have been estimated to account for up to 12% of the total sulfur
47 mass in fine particles, playing significant roles in the global biogeochemical cycling
48 of sulfur (Luk'Acs et al. 2009). In particular, OSs can impact the properties of
49 aerosols, such as hygroscopicity, acidity, viscosity, and morphology, which are closely
50 associated with the organic aerosol formation and urban air quality (Riva et al. 2019;
51 Fleming et al. 2019). Thus, aerosol OSs have attracted significant attention over the
52 years. However, the mechanisms and key factors impacting the formation and
53 abundance of aerosol OSs in the real world remain considerable uncertainty, despite
54 the important insights gained from laboratory simulation experiments (Wang et al.
55 2021; Yang et al. 2023; Wang et al. 2020).

56 Previous field studies have indicated that acidity (Duporté et al. 2019), sulfate
57 (Aoki et al. 2020), aerosol liquid water (Duporté et al. 2016), and oxidants (e.g.,
58 ozone) (Wang et al. 2021) represent critical factors controlling the formation of OSs
59 via heterogeneous and liquid phase processes (Brüggemann et al. 2020b). Precursor
60 emission intensities (e.g., isoprene, monoterpenes, polycyclic aromatic hydrocarbons,
61 and alkanes) also play an important role in impacting abundance of biogenic and
62 anthropogenic OSs in ambient aerosols (Wang et al. 2022; Bryant et al. 2021; Yang et
63 al. 2024). Furthermore, previous studies have identified a large number of CHOS
64 compounds in smoke particles (e.g., pine branches, corn straw, rice straw, and coal)

65 (Song et al. 2019; Song et al. 2018; Tang et al. 2020). However, limited studies have
66 focused on the contribution of different smoke particles to urban aerosol OSs. This
67 may be an overlooked source of OSs. In general, few field studies have conducted a
68 comprehensive investigation into the relationship between biogenic and
69 anthropogenic impacting factors and regional differences in aerosol OS pollution.
70 **This complicates our understanding of how aerosol OS pollution is formed and what**
71 **limits it in a complex polluted atmosphere across different cities in China.**

72 The considerable variations in climatic conditions and air pollution levels in the
73 northern and southern regions of China during winter (Ding et al. 2014; Ding et al.
74 2016b) provide a distinctive opportunity to examine the complex influences of
75 precursors, humidity, acidity, atmospheric oxidants, and anthropogenic pollution on
76 the formation and abundance of aerosol OSs in the real world (Yang et al. 2024; Yang
77 et al. 2023; Wang et al. 2021; Hettiyadura et al. 2019). In this study, we conducted the
78 simultaneous observations of OSs and other chemical components in PM_{2.5} collected
79 from typical southern (Guangzhou and Kunming) and northern (Xi'an and Taiyuan)
80 cities in China during winter. Moreover, we also attempted to identify OSs in smoke
81 particles emitted from combustion of different materials (i.e., rice straw, pine branch,
82 diesel, gasoline, and coal). The principal aims of this study are 1) to investigate the
83 spatial differences in aerosol OS pollution in northern and southern China during
84 winter and 2) to elucidate the key factors that contribute to the spatial variability of
85 OS pollution, with a focus on the OSs derived from smoke particles.

86

87 **2. Materials and Methods**

88 **2.1. Site description and sample collection**

89 The research sites are located in four urban areas in China, including Xi'an (XA)
90 Taiyuan (TY), Guangzhou (GZ), and Kunming (KM) (**Figure S1a**). XA and TY are
91 typical northern cities with cold winters (average temperature below 2 °C during the
92 study period; **Table S1**). Thus, burning coal and biomass for heating is prevalent in
93 these two cities during winter (Zhou et al. 2017; Ma et al. 2017), which significantly
94 deteriorated the local air quality (**Figure S1b**). GZ and KM represent typical southern
95 cities, with an average air temperature of over 10 °C during the winter sampling
96 period (**Table S1**). Clearly, the distinctive climatic conditions in the northern and
97 southern cities during winter may lead to significant spatial differences in the level of
98 air pollution and the emission intensity of biogenic volatile organic compounds
99 (VOCs) (Ding et al. 2014; Xu et al. 2024b).

100 From 10 December 2017 to 8 January 2018, sampling was performed
101 simultaneously in four cities. Filters contained PM_{2.5} were collected at regular two- to
102 three-day intervals, with the collection duration being 24 hours, using a high-volume
103 air sampler (Series 2031, Laoing, China) at a flow rate of \sim 1.05 m³ min⁻¹ (Xu et al.
104 2024a). A blank filter was sampled at each of the study sites. **A total of 48 ambient**
105 **samples** were collected and stored at a temperature of -30°C . Meteorological data,
106 including wind speed, relative humidity (RH), and temperature, were obtained from
107 nearby environmental stations. Concurrently, the concentrations of various pollutants,
108 such as O₃, NO₂, and SO₂, were also recorded.

109 **2.2. Smoke particle collection**

110 The controlled burning experiments conducted in the field were designed to
111 simulate the emissions of “real world” burning cases in China (**Figure S2**), with the
112 methodology being improved according to the previous reports (He et al. 2010; Wang
113 et al. 2017). Rice straw and pine branch are typical materials for biomass burning in
114 China (Zhou et al. 2017). In addition, the combustion of coal, gasoline, and diesel was
115 representative of fossil fuel combustion (Yu et al. 2020). Accordingly, the smoke
116 particles emitted from rice straw, pine branch, coal combustion, gasoline vehicle
117 exhausts, and diesel vehicle exhausts were separately collected using self-made
118 devices (**Figure S2**).

119 Briefly, the smoke from the combustion of rice straw, pine branch, and coal was
120 sampled through a combustion furnace pumped with ambient air (particulate matter is
121 removed) (**Figure S2a**). It should be noted that introducing ambient air with removed
122 particulate matter into the combustion furnace is to minimize the pollution of ambient
123 particulate matter to the smoke particle samples. Each combustion experiment for
124 straw, pine branch, and coal lasted for 30–40 min. Regarding the smoke particles
125 emitted from gasoline vehicle exhausts and diesel vehicle exhausts, they were
126 collected for 3 hours by directly connecting to the car exhaust pipe (**Figure S2b**). All
127 smoke particle samples are collected onto prebaked quartz fiber filters via a high-
128 volume air sampler (Series 2031, Laoing, China). Four repeated experiments were
129 conducted for each combustion material, one of which was collected as a blank
130 sample. All smoke particle samples were stored at -30°C .

131 **2.3. Chemical analysis and predictions of aerosol acidity and water concentration**

132 The extraction, measurement procedures, and identification of OSs were
133 described in detail in our recent publications (Yang et al. 2024). Briefly, the filter
134 sample was extracted using methanol, then filtered through a 0.22 μm PTFE syringe
135 filter and concentrated by a gentle stream of nitrogen gas. Subsequently, the
136 concentrated sample with adding ultrapure water (300 μL) was thoroughly mixed
137 using a mixer. The mixture was centrifuged to obtain the supernatant for analysis of
138 UPLC-MS/MS system (Waters, USA) (Wang et al. 2021). **The reverse-phase liquid**
139 **chromatography (RPLC) method was performed on an Acquity UPLC HSS T3**
140 **column (2.1mm \times 100 mm, 1.8 μm particle size; Waters, USA)** in this study. Although
141 our method is quite effective in retaining and separating low molecular weight (MW)
142 OSs, as demonstrated in our recent publication (Yang et al. 2024), **we also**
143 **acknowledge that the developed hydrophilic interaction liquid chromatography**
144 **method may provide another solution for the measurement of low-MW OSs** (Cui et al.
145 2018; Hettiyadura et al. 2015).

146 **In addition**, it has been indicated in previous studies (Brüggemann et al. 2020a;
147 Kristensen et al. 2016) that the levels of OSs can be affected by the sampling
148 procedure, especially when SO_2 removal procedures are not employed. On the
149 assumption that SO_2 reacts with organics on filters to form OSs, similar processes
150 must also occur on ambient particles prior to sampling. **Moreover**, there is currently
151 no study evaluating the relative efficiency of OS generation in filters and ambient
152 particles. **Consequently, the possible consequences of sampling without denuding SO_2**

153 for the quantification of OSs were not taken into account in our studies (Yang et al.
154 2024; Yang et al. 2023). In total, 212 OSs were identified. However, only 111 OS
155 species were quantified using surrogate standards in this study (**Table S2** and **S3**). The
156 study divided the several principal OS groups as follows: monoterpene-derived OSs
157 (OS_m), isoprene-derived OSs (OS_i), C₂–C₃ OSs (i.e., OSs with two or three carbon
158 atoms), and anthropogenic OSs (i.e, aliphatic and aromatic OSs) (Yang et al. 2023).
159 The terms "OS_m" and "OS_i" refer to organosulfates generated from monoterpene and
160 isoprene, respectively. These compounds were generally classified as biogenic OSs
161 due to their natural origin (Wang et al. 2021; Wang et al. 2018). The specific
162 classification and quantification methods were detailed in our recent publications
163 (Yang et al. 2023; Yang et al. 2024) and **Supporting Information**.

164 An additional portion of each filter was extracted using ultrapure water for
165 determining the inorganic ions (Huang et al. 2023). The concentrations of SO₄²⁻, Ca²⁺,
166 NO₃⁻, Na⁺, K⁺, Mg²⁺, Cl⁻, and NH₄⁺ were analyzed using ICS5000+ ion
167 chromatography (Thermo, USA) (Yang et al. 2024; Lin et al. 2023). The mass
168 concentration of aerosol liquid water (ALW) and pH value were calculated by a
169 thermodynamic model (ISORROPIA-II) in the forward mode and thermodynamically
170 metastable state, which was detailed in our previous studies (Liu et al. 2023; Xu et al.
171 2022; Xu et al. 2023b; Xu et al. 2020). The influence of OSs on ALW and pH was not
172 taken into account in the present study due to their negligible contribution to the
173 prediction outcomes, as indicated by Riva et al. (2019) and Yang et al. (2024).

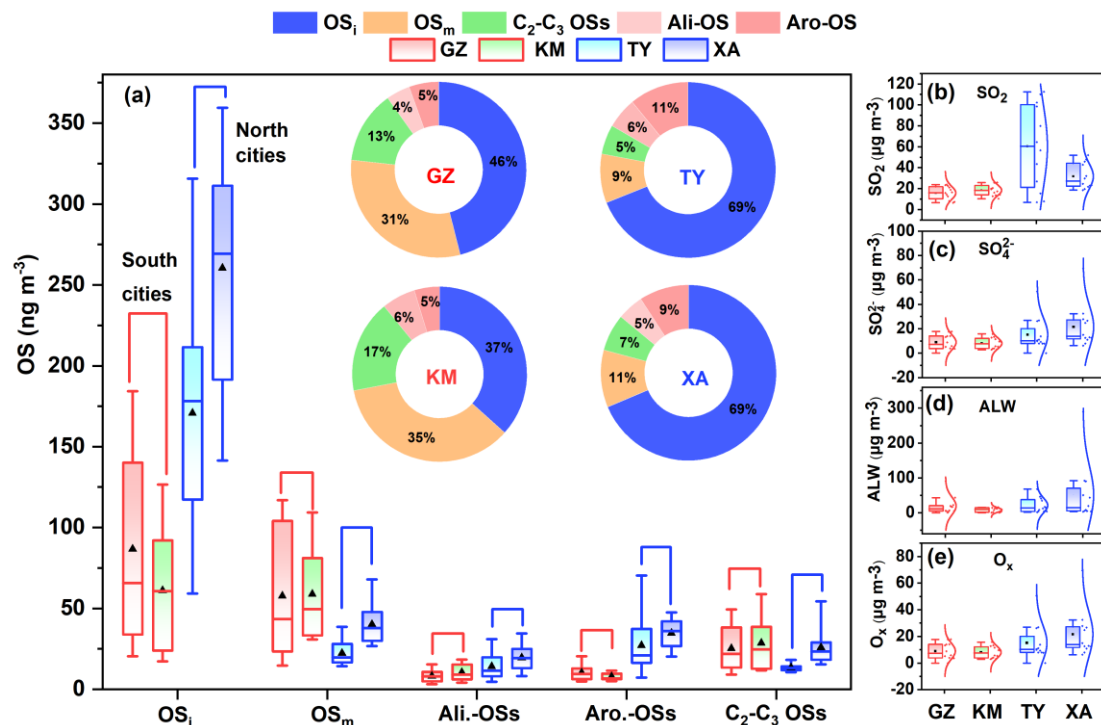
174

175 **3. Results and Discussion**

176 **3.1. Spatial variations in concentrations and compositions of different OSs**

177 **Figure 1a** shows the spatial distributions in mass concentrations and mass
178 fractions of OS_i, OS_m, aliphatic OSs, aromatic OSs, and C₂–C₃ OSs in PM_{2.5} collected
179 in southern (KM and GZ) and northern (TY and XA) cities during winter. On average,
180 OS_i was the dominant OS subgroup, which accounted for 37% – 46% and 68% – 69%
181 of the total OS mass in southern and northern cities, respectively. The predominance
182 of OS_i in aerosol OSs was also reported by previous studies in cities in northern (e.g.,
183 Beijing and Tianjin) (Wang et al. 2018; Ding et al. 2022) and southern (e.g.,
184 Guangzhou and Shanghai) (Wang et al. 2022; Wang et al. 2021) China, as well as in
185 coastal (the Yellow Sea and Bohai Sea) (Wang et al. 2023) and European (Sweden)
186 (Kanellopoulos et al. 2022) and American regions (Chen et al. 2021; Hettiyadura et al.
187 2017; Hettiyadura et al. 2019) (**Table S4**). Moreover, the concentrations of OS_i were
188 significantly lower in southern cities ($61 \pm 38 \text{ ng m}^{-3}$ – $87 \pm 60 \text{ ng m}^{-3}$) than in
189 northern cities ($171 \pm 69 \text{ ng m}^{-3}$ – $260 \pm 71 \text{ ng m}^{-3}$) (**Table S1**), showing a
190 concentration range overlapped with previous observations (**Table S4**). From southern
191 to northern cities, the mass concentrations and mass fractions of OS_m tended to
192 decrease, which was opposite to the spatial variation pattern of OS_i (**Figure 1a**). Both
193 OS_i and OS_m are generally considered as typical biogenic OSs (Hettiyadura et al.
194 2019; Wang et al. 2018), the abundances of which were tightly associated with
195 biogenic VOC emissions when **acidity, sulfate, atmospheric oxidation capacity**, and
196 ALW are not limiting factors (Bryant et al. 2021; Wang et al. 2022; Yang et al. 2024).

197 Thus, these dissimilarities in the spatial variations of OS_i and OS_m can be attributed to
 198 large differences in the intensity of biogenic VOC emissions (Wang et al. 2022)
 199 and/or the key factors that constrain OS formation between the northern and southern
 200 regions of China (**Table S1**).



201 **Figure 1** Box and whisker plots showing the variations in the concentration of
 202 different OS groups in PM_{2.5} collected in southern (GZ and KM) and northern (TY
 203 and XA) cities of China during winter. Each box encompasses the 25th–75th
 204 percentiles. Whiskers are the minimum and maximum values. The triangles and solid
 205 lines inside boxes indicate the mean and median. The spatial variation in average
 206 abundance of anthropogenic OSs (i.e., OS_a, including aliphatic and aromatic
 207 OSs) was also shown in panel (a). The other figures show the spatial variations in (b) SO₂, (c) SO₄²⁻, (d) ALW, and (e) O_x levels.

209

210 The abundance of anthropogenic OSs (i.e., OS_a, including aliphatic and aromatic

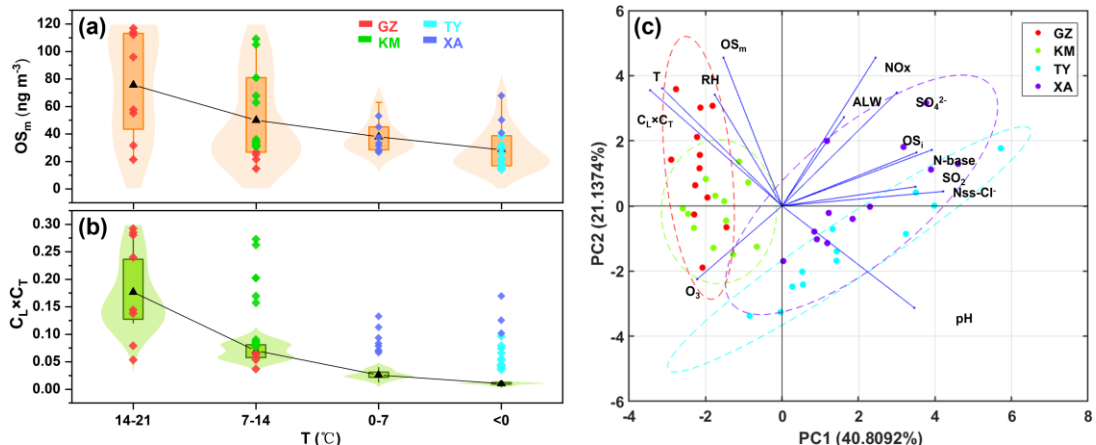
211 OSs, **Sect. S1**) in southern cities was lower than that of OS_m , which was opposite to
212 the case in the northern cities showing higher anthropogenic OS abundance (**Figure**
213 **1a** and **Table S1**). Moreover, we found that the spatial variation patterns of OS_i and
214 OS_a were similar to those of SO_2 , SO_4^{2-} , ALW, and O_x (**Figures 1b–e**), as indicated by
215 significant ($P < 0.05$) correlations of OS_i and OS_a with those factors (**Figure S3**).
216 However, OS_m and $C_2–C_3$ OSs showed the opposite spatial variation pattern to SO_2 ,
217 SO_4^{2-} , ALW, and O_x (**Figure 1**). If both OS_i and OS_m are assumed to be formed mainly
218 from the oxidation of biologically emitted VOCs, the higher SO_2 , SO_4^{2-} , ALW, and O_x
219 levels could theoretically lead to higher OS_m in northern cities, just as these factors
220 leaded to higher OS_i abundance in northern cities (**Figure 1** and **Table S1**).
221 Accordingly, the above differentiated spatial variation patterns among different OS
222 subgroups likely indicated that other sources of isoprene contributed to the formation
223 of OS_i in northern cities. Further given the significant ($P < 0.05$) correlations between
224 OS_i and OS_a , non biogenic isoprene emissions may play an important role in the
225 formation of aerosol OS_i in northern cities. This will be further demonstrated in the
226 following discussion.

227

228 **3.2. Key factors affecting spatial differences in monoterpane-derived OS**
229 **abundance**

230 **Figure 2a** shows the distribution of OS_m concentration as a function of air
231 temperature. We found that the OS_m concentration tended to increase with the increase
232 of air temperature. Specifically, the air temperature in the southern cities was mainly

233 in the range of 7–14°C during the sampling period, corresponding to higher aerosol
234 OS_m abundance. In contrast, the low temperature (< 7°C) in the northern cities
235 corresponded to a significant decrease in OS_m abundance. This finding was similar to
236 the previously observed decrease in aerosol OS_m compounds with decreasing
237 temperature during winter in Guangzhou (Bryant et al. 2021). Furthermore, the
238 indicator (C_L × C_T) of biogenic VOC emission rate (Ding et al. 2016a; Guenther et al.
239 1993) was also higher in southern cities than in northern cities (Figure 2b), which
240 implied higher monoterpene emissions in southern cities. It has been suggested that
241 the emission rates of biogenic VOCs (e.g., monoterpene and isoprene) can be driven
242 by increased air temperature and lighting (Ding et al. 2016a; Ding et al. 2016b). A
243 previous study also found that the concentrations of atmospheric monoterpenes during
244 the winter season were higher in warmer southern Chinese cities than in colder
245 northern Chinese cities (Ding et al. 2016b; Li et al. 2020). In particular, GZ and KM,
246 which encompass extensive areas of coniferous and broad-leaved forests, have been
247 identified as hotspots for monoterpene and isoprene emissions (Li and Xie 2014).
248 Considering the lower levels of key factors affecting OS formation observed in
249 southern cities (Figures 1b–e and Table S1), it can be inferred that the significant
250 spatial differences in OS_m abundances were largely attributed to temperature
251 dependent emission of monoterpenes.



252

253 **Figure 2** Distribution of (a) OS_m and (b) $C_L \times C_T$ data in different temperature ranges
 254 during winter. The triangles inside boxes indicate the mean. Principal component
 255 analysis result (c) deciphering the relationship among OS_i , OS_m , and key factors
 256 influencing OS formation.

257

258 To further determine the key factors affecting the spatial differences of OS_m ,
 259 principal component analysis was conducted (**Figure 2c**). It can be easily determined
 260 that the abundance of aerosol OS_m was closely related to changes in air temperature
 261 and $C_L \times C_T$ value. **This further explained the changes** in OS_m data in the southern
 262 cities. In contrast, the abundance of aerosol OS_i in the northern cities was more
 263 influenced by anthropogenic factors, as indicated by combustion source tracers such
 264 as nitrogen-containing bases (N-bases) and non-sea-salt Cl^- (nss- Cl^-) (Wang et al.
 265 2017; Jiang et al. 2023) (**Figure 2c**). Thus, principal component analysis can perfectly
 266 distinguish the main factors causing changes in OS_m and OS_i abundances between the
 267 northern and southern cities. In general, the above results confirm that the spatial
 268 variation of OS_m was predominantly controlled by temperature-related monoterpane

269 emissions. However, this cannot account for the observed spatial variation of OS_i
270 (**Figure 2c and Figure S4**). Interestingly, the spatial distribution patterns of OS_m and
271 OS_i in northern and southern China exhibited consistency during summer, closely
272 resembling the spatial distribution of biogenic VOC emission intensities (Wang et al.
273 2022). Thus, this case together with our observations during winter further imply that
274 non biogenic sources of isoprene were important contributors to the formation of OS_i
275 in northern China during winter.

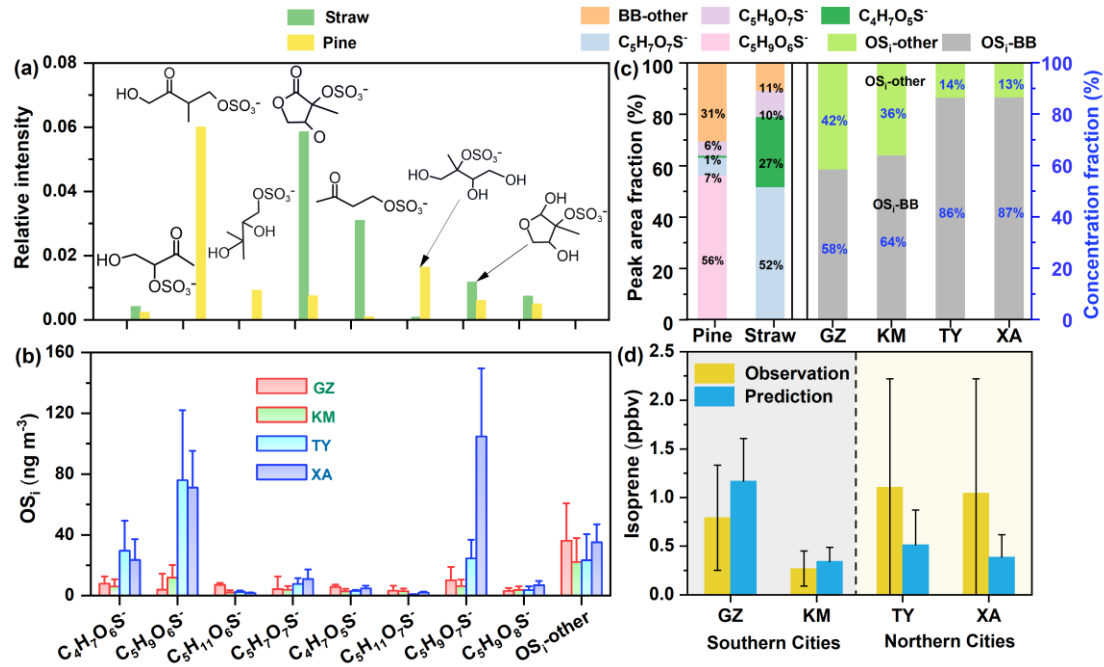
276

277 **3.3. Significant contribution of biomass burning to isoprene-derived OSs in**
278 **Northern China**

279 The previous principal component analysis has suggested that the abundance of
280 OS_i in northern cities was closely related to the levels of combustion source tracers
281 (e.g., N-base compounds and nss-Cl⁻). N-base compounds are CHN species that
282 contain exclusively C, H, and N atoms, and have been demonstrated to exhibit high
283 sensitivity as molecular indicators in identifying biomass burning (Wang et al. 2017).

284 To further confirm the potential contribution of combustion release to aerosol OS_i,
285 OSs in smoke particles emitted from rice straw, pine branch, and coal combustion, as
286 well as from gasoline vehicle exhausts, and diesel vehicle exhausts (**Figure S2**), were
287 investigated. A total of 8 distinct OS_i were identified in both the smoke particles
288 emitted from biomass burning (rice straw and pine branch) and the ambient aerosol
289 particles, including C₄H₇O₆S⁻, C₅H₉O₆S⁻, C₅H₁₁O₆S⁻, C₅H₇O₇S⁻, C₄H₇O₅S⁻,
290 C₅H₁₁O₇S⁻, C₅H₉O₇S⁻, and C₅H₉O₈S⁻. Moreover, the peak intensities of these 8 OS_i

291 in smoke particles emitted from fossil fuel combustion (gasoline and diesel vehicle
292 exhausts and coal) were close to those in the blank sample. A previous investigation
293 into CHOS compounds in smoke particles emitted from residential coal combustion
294 and biomass burning also failed to identify OS_i species (Song et al. 2019; Song et al.
295 2018), which further supported the reliability of the combustion experiment
296 conducted in this study. C₅H₉O₆S⁻ was dominant OS_i species in pine-derived smoke
297 particles (**Figure 3a,c**). We found that the average concentration of C₅H₉O₆S⁻ in
298 ambient aerosol samples was much higher in northern cities than in southern cities
299 (**Figure 3b**). A reasonable explanation for this is that pine branches are commonly
300 used as solid fuel for heating and cooking in northern suburbs and rural areas (Zhou et
301 al. 2017). C₅H₇O₇S⁻ and C₄H₇O₅S⁻ dominated OS_i species in straw-derived smoke
302 particles (**Figure 3a,c**). However, these two types of OS_i have relatively low
303 abundance in ambient aerosol samples in both northern and southern cities. This may
304 be attributed to the fact that straw burning was mainly concentrated in autumn rather
305 than winter in China (Zhou et al. 2017; Yang et al. 2015). On average, the biomass
306 burning-related OS_i accounted for 58% – 64% and 86% – 87% of the total OS_i
307 concentration in southern and northern cities, respectively (**Figure 3c**). Although
308 these biomass burning-related OS_i can also be formed through atmospheric
309 transformation of biogenic isoprene, the higher proportion of these OS_i in northern
310 cities together with previous principal component analysis results still support our
311 previous consideration that non biogenic OS_i may be an important contributor to
312 aerosol OS_i in northern cities.



313

314 **Figure 3** Relative signal intensity of (a) identified major OS_i species in different types
 315 of smoke particle samples. Spatial variation in the concentration of several specific
 316 OS_i (identified in smoke particles) in (b) ambient PM_{2.5} samples. Peak area and
 317 concentration fraction of (c) OS_i species identified in both ambient PM_{2.5} samples
 318 collected in different cities and smoke particles. Comparison of (d) isoprene mixing
 319 ratios obtained from observation and modeling in different cities (Zhang et al. 2020).

320

321 Previous laboratory studies have suggested that these identified OS_i species in
 322 biomass burning-derived smoke particles are typically formed through heterogeneous
 323 and multiphase reactions involving isoprene, its oxidation intermediates, and sulfate
 324 or sulfur dioxide (Surratt et al. 2008; Surratt et al. 2007; Darer et al. 2011).
 325 Specifically, C₅H₉O₆S⁻, as a sulfate ester of C₅-alkene triols, was formed mainly
 326 through the uptake of gas-phase isoprene oxidation products onto acidified sulfate
 327 aerosol (Surratt et al. 2007). The formation of C₅H₇O₇S⁻ and C₅H₉O₇S⁻ begins with

328 the gas-phase oxidation of isoprene (Surratt et al. 2008). $\text{C}_4\text{H}_7\text{O}_6\text{S}^-$ can be generated
329 both from isoprene photooxidation and sulfate radical reaction with methacrolein
330 (MACR) or methyl vinyl ketone (MVK) (Schindelka et al. 2013; Wach et al. 2019;
331 Nozière et al. 2010). $\text{C}_5\text{H}_{11}\text{O}_7\text{S}^-$ was produced by reactive uptake of isoprene-derived
332 epoxide (IEPOX) on sulfate under low-NO_x conditions. **Since our combustion**
333 **experiments have excluded the direct contribution of ambient aerosol particles to OS_i**
334 **in smoke particles, it can be expected that these detected OS_i compounds were mainly**
335 **generated within smoke plumes through the isoprene oxidation pathway mentioned**
336 **above. It has been demonstrated that directly emitted organic aerosols or VOCs can**
337 **undergo a chemical reaction within smoke plumes, forming secondary organic**
338 **compounds within a matter of hours** (Wang et al. 2017; Song et al. 2018; Mason et al.
339 2001). A field study conducted by Zhu et al. (2016) at a rural site (Yucheng) in the
340 North China Plain (NCP) region has observed that the concentration of ambient
341 isoprene during the period of straw combustion was approximately twice as high as
342 that observed during periods of non combustion. In addition, Li et al. (2018) found
343 that isoprene-derived epoxides increased significantly during field open burning of
344 straw. Generally, despite the fact that a few of the mechanisms by which OSs are
345 formed have been verified through field studies, the formation of CHOS and CHONS
346 compounds has been observed to occur in the biomass burning plume (Zhang et al.
347 2024; Song et al. 2018; Tang et al. 2020). Thus, these previous case studies further
348 support our consideration that OS_i compounds formed in biomass burning-derived
349 smoke particles in this study can be attributed to increasing isoprene emission caused

350 by field biomass burning (Zhu et al. 2016) and favorable aqueous secondary organic
351 aerosols (SOA) formation during the aging process of the biomass burning plume
352 (Gilardoni et al. 2016).

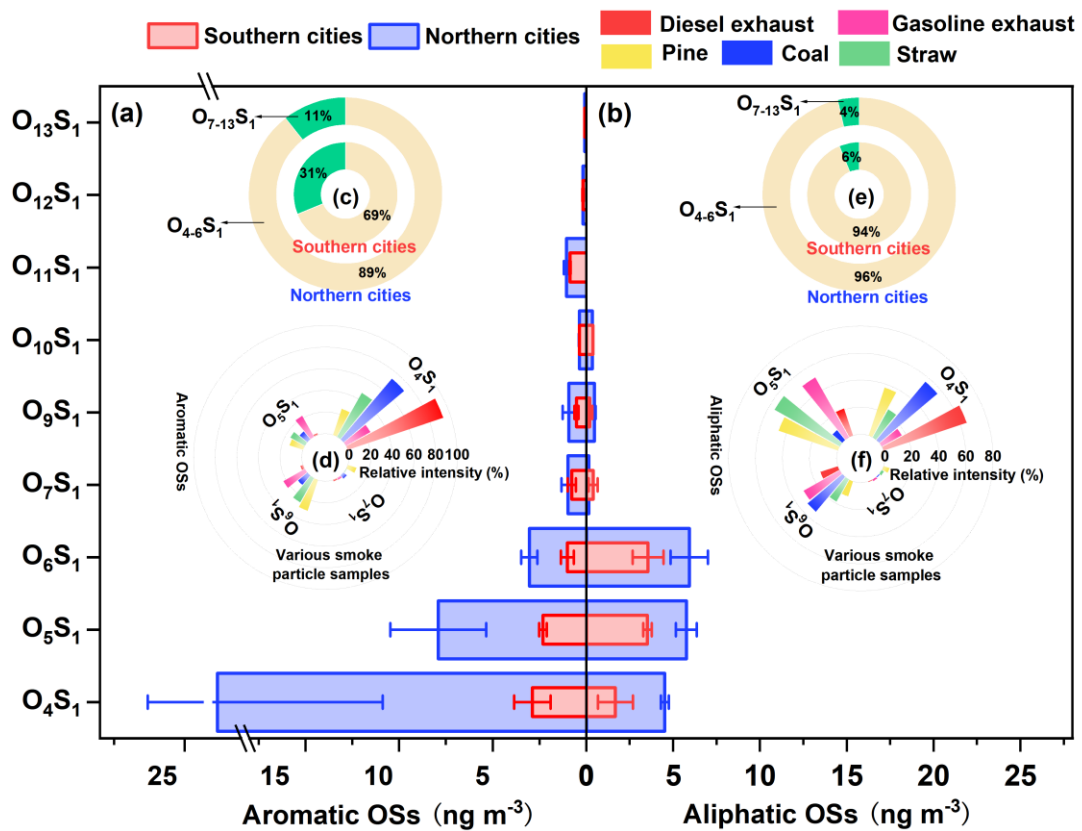
353 **Figure 3d** presents a comparison between the isoprene mixing ratios derived
354 from model simulations (plant functional type related model) and those observed in
355 the field in different Chinese cities during winter (December and January) (Zhang et
356 al. 2020). Overall, the levels of isoprene observed in northern cities during winter
357 were higher than those in southern cities. In addition, the predicted values in southern
358 cities were slightly higher than the observed values, which may be attributed to the
359 lag in model prediction results caused by the rapid urbanization rates in these southern
360 cities (Zhang et al. 2020). However, the observed values in these two northern cities
361 were 53% to 63% higher than the predicted values, on average. Clearly, this plant
362 functional type related isoprene prediction model cannot explain the large amount of
363 “missing” isoprene sources in northern cities. Thus, the observed spatial differences in
364 OS_i (**Figure 1**) and field combustion experiments (**Figure 3**) can suggest that these
365 “missing” isoprene sources were mainly derived from biomass burning, significantly
366 contributing to the production of aerosol OS_i in northern cities. **This can also be**
367 supported by previous principal component analysis involving combustion source
368 tracers and OS_i compounds (**Figure 2c**).

369

370 **3.4. Formation of anthropogenic OSs mainly driven by fossil fuel and biomass**
371 **combustion**

372 **Figures 4a,b** show the average concentration distribution of anthropogenic OSs
373 classified based on the number of O atoms in their molecules in southern (GZ and
374 KM) and northern (TY and XA) cities. The O₄S₁ subgroup was the most abundant
375 aromatic OSs in both southern and northern cities, among which C₉H₉O₄S⁻, phenyl
376 sulfate (C₆H₅O₄S⁻), and benzyl sulfate (C₇H₇O₄S⁻) were dominant species (**Table S3**).
377 C₇H₇O₄S⁻ and C₆H₅O₄S⁻ have been suggested to be formed mainly through the
378 photooxidation of 2-methylnaphthalene and naphthalene (Riva et al. 2015), or
379 alternatively, by the sulfate radical reaction with aromatic compounds, including
380 toluene and benzoic acid, in an aqueous phase environment (Riva et al. 2015). The
381 formation mechanism of C₉H₉O₄S⁻ is rarely reported. However, C₉H₉O₄S⁻, C₆H₅O₄S⁻,
382 and C₇H₇O₄S⁻ were also detected in both fossil fuel combustion-derived smoke
383 particles and biomass burning-derived smoke particles (**Figure S5** and **Table S5**),
384 indicating that the aromatic VOCs produced by fuel combustion are closely related to
385 the formation of these aromatic OSs. Overall, aerosol aromatic OS compounds in both
386 southern and northern cities were mainly distributed between four and six O atoms
387 (**Figure 4c**), which was similar to the distribution of aromatic OSs identified in
388 various smoke particles emitted from different combustion sources (**Figure 4d**).
389 However, the average abundances of aromatic O₄₋₆S₁ compounds in northern cities
390 were 3–6 times higher than those in southern cities. The above results suggest that
391 aromatic OSs originated from fossil fuel and biomass combustion activities are
392 important contributors to urban aerosol anthropogenic OSs in winter in China,
393 especially in northern cities. We found that the correlations between aromatic OSs and

394 anthropogenic indicators (SO_2 , SO_4^{2-} , N-base, and nss- Cl^-) were stronger in northern
 395 cities than in southern cities (**Figure S6**), and that the release of polycyclic aromatic
 396 hydrocarbons from fossil fuel combustion was also higher in northern cities (**Figure**
 397 **S7**). This further indicates that higher aerosol aromatic OSs in northern cities was
 398 mainly attributed to stronger combustion activities in those cities.



399
 400 **Figure 4** Concentration distribution of different (a) aromatic and (b) aliphatic OS
 401 subgroups (classification based on oxygen atoms) in southern and northern cities.
 402 Ring charts (c,e) show the percentage contributions of O_{4-6}S_1 and $\text{O}_{7-13}\text{S}_1$ subgroups.
 403 Radial bar charts (d,f) illustrate the relative signal intensity of different OS subgroups
 404 in different smoke particle samples.

405

406 Aliphatic OSs were also predominantly distributed between O_4S_1 and O_6S_1

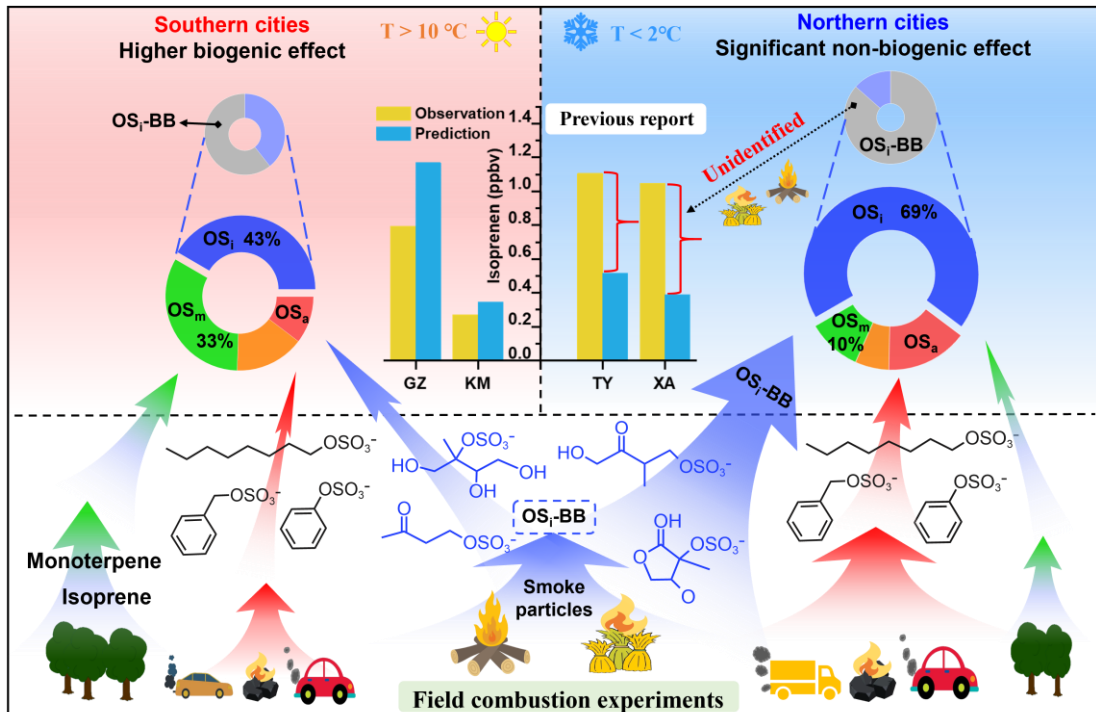
407 subgroups in both southern and northern cities (**Figures 4b,e**), which was similar to
408 the case found in both fossil fuel combustion-derived smoke particles and biomass
409 burning-derived smoke particles (**Figure 4f**). It has been suggested that the long-chain
410 alkanes derived from traffic emissions can largely contribute to the formation of
411 CHOS compounds with aliphatic carbon chains (Tao et al. 2014). In addition, Tang et
412 al. (2020) analyzed the molecular compositions of smoke particles from open biomass
413 burning, household coal combustion and vehicle emissions and suggested that the
414 aliphatic CHOS compounds can be derived from both vehicle emissions and coal and
415 biomass combustion. In this study, aliphatic OSs showed a significant ($P < 0.05$)
416 positive correlation with nss-Cl⁻, SO₂, NO_x, and N-base compounds in both southern
417 and northern cities (**Figure S6 and S8**), indicating aerosol aliphatic OSs were affected
418 by a combination of biomass burning and vehicle emissions in those cities during
419 winter. Thus, the significantly higher level of aliphatic O₄₋₆S₁ species in northern
420 cities indicated that the formation of aliphatic OSs in northern cities was more driven
421 by pollutants released from the combustion of fossil fuels and biomass compared to
422 southern cities. This consideration is highly consistent with the fact that the
423 concentrations of air pollutants (e.g., SO₂ and NO₂) in northern cities with a large
424 demand for heating during winter are usually higher than those in warmer southern
425 cities (**Table S1 and Figure S1b**) (Yu et al. 2020; Ding et al. 2017; Ma et al. 2017;
426 Zhou et al. 2017).

427

428 **4. Conclusion and atmospheric implications**

429 It has been previously suggested that isoprene can also be released into the
430 atmosphere as a result of open burning of agricultural residues and forest fires
431 (Andreae 2019; Simpson et al. 2011). A field study conducted by (Wang et al. 2019)
432 in Beijing during winter inferred that the prevalence of OS_i compounds in total
433 aerosol OSs may be partially attributable to biomass burning emissions, although
434 there was a paucity of compelling evidence to support this hypothesis. This work
435 combines strongly contrasting observational studies (northern Chinese Cities vs
436 southern Chinese Cities) with in situ combustion modelling experiments to provide
437 the first direct evidence that biomass burning emission, rather than fossil fuel
438 combustion emission, is a significant contributor to aerosol OS_i in northern cities
439 (**Figure 5**). In Chinese cities, particularly those in the northern region, biomass
440 materials are extensively utilized for domestic heating and cooking purposes during
441 the winter season (Zhou et al. 2017). Clearly, the isoprene emissions from biomass
442 combustion sources would result in higher isoprene mixing ratios than those
443 simulated by the model (Zhang et al. 2020) that only considers natural isoprene
444 emissions. Thus, isoprene prediction models applied to Chinese winters in the future
445 should also take into account the various biomass combustion source releases. **Given**
446 **the potential for both biomass burning and biogenic isoprene to contribute to OS_i**
447 **formation, separating their respective contributions remains challenging.** Furthermore,
448 biogenic OSs are important SOA constituents and have been frequently serve as
449 important tracers for biogenic SOA (Ding et al. 2014; Ding et al. 2016a). The overall
450 results suggest that some OS_i species may not be suitable as biogenic SOA markers,

451 especially in areas with intensive biomass burning activities, such as northern Chinese
 452 cities during winter.



453
 454 **Figure 5** Conceptual picture showing the characteristics and main contributors of OSs
 455 in northern and southern China during winter. It is noteworthy that OS_i -BB can
 456 originate not only from biomass combustion, but also from the secondary formation
 457 of isoprene emitted from biogenic sources.

458
 459 We found that different fossil fuel combustion emissions (e.g., vehicle emissions
 460 and coal combustion emissions) and biomass burning emissions can contribute to
 461 aerosol anthropogenic OSs. However, current studies have not been able to accurately
 462 distinguish between the contributions of various material combustion to different
 463 types of anthropogenic OSs. Future research is necessary to develop more
 464 comprehensive models to further explore the effects of various combustion sources on

465 the generation and reduction of urban aerosol OS pollution. Of particular importance
466 is that although the production of various OSs was directly observed through our
467 simulated combustion experiments, it is not clear whether the chemical mechanisms
468 involved are similar to those derived from the laboratory simulations. This is because
469 the combustion process is accompanied by the effects of high temperatures. In
470 general, although our results provide direct evidence for the release of OSs from
471 combustion of various combustion sources, further mechanistic studies and
472 environmental impact assessment are still urgently needed. This may be important for
473 effective control of urban wintertime organic aerosol pollution in China.

474

475 **Data availability**

476 The data presented in this work are available upon request from the corresponding
477 authors.

478

479 **Competing interests**

480 The authors declare no conflicts of interest relevant to this study.

481

482 **Author contributions**

483 YX designed the study. TY, YJM, HWX, and HX performed field measurements and
484 sample collection; TY and YJM performed chemical analysis; YX and TY performed
485 data analysis; YX and TY wrote the original manuscript; and YX, TY, YCW, and
486 HYX reviewed and edited the manuscript.

487

488 **Acknowledgements**

489 The authors are very grateful to Jian-Zhen Yu at the Hong Kong University of Science
490 and Technology for her kind and valuable comments to improve the paper.

491

492 **Financial support**

493 This study was kindly supported by the National Natural Science Foundation of China
494 (grant number 42303081, 42373083, and 22306059), the Shanghai “Science and
495 Technology Innovation Action Plan” Shanghai Sailing Program (grant number
496 22YF1418700), and the National Key Research and Development Program of China
497 (grant number 2023YFF0806001).

498

499

500

References

502 Andreae, M. O.: Emission of trace gases and aerosols from biomass burning – an updated assessment,
503 *Atmos. Chem. Phys.*, 19, 8523-8546, 10.5194/acp-19-8523-2019, 2019.

504 Aoki, E., Sarrimanolis, J. N., Lyon, S. A., and Elrod, M. J.: Determining the Relative Reactivity of
505 Sulfate, Bisulfate, and Organosulfates with Epoxides on Secondary Organic Aerosol, *ACS Earth*
506 *Space Chem.*, 4, 1793-1801, 10.1021/acsearthspacechem.0c00178, 2020.

507 Brüggemann, M., Riva, M., Perrier, S., Poulain, L., George, C., and Herrmann, H.: Overestimation of
508 Monoterpene Organosulfate Abundance in Aerosol Particles by Sampling in the Presence of SO₂,
509 *Environ. Sci. Technol. Lett.*, 8, 206-211, 10.1021/acs.estlett.0c00814, 2020a.

510 Brüggemann, M., Xu, R., Tilgner, A., Kwong, K. C., Mutzel, A., Poon, H. Y., Otto, T., Schaefer, T.,
511 Poulain, L., Chan, M. N., and Herrmann, H.: Organosulfates in Ambient Aerosol: State of
512 Knowledge and Future Research Directions on Formation, Abundance, Fate, and Importance,
513 *Environ. Sci. Technol.*, 54, 3767-3782, 10.1021/acs.est.9b06751, 2020b.

514 Bryant, D. J., Elzein, A., Newland, M., White, E., Swift, S., Watkins, A., Deng, W., Song, W., Wang, S.,
515 Zhang, Y., Wang, X., Rickard, A. R., and Hamilton, J. F.: Importance of Oxidants and Temperature
516 in the Formation of Biogenic Organosulfates and Nitrooxy Organosulfates, *ACS Earth Space*
517 *Chem.*, 5, 2291-2306, 10.1021/acsearthspacechem.1c00204, 2021.

518 Chen, Y., Dombek, T., Hand, J., Zhang, Z., Gold, A., Ault, A. P., Levine, K. E., and Surratt, J. D.:
519 Seasonal Contribution of Isoprene-Derived Organosulfates to Total Water-Soluble Fine Particulate
520 Organic Sulfur in the United States, *ACS Earth Space Chem.*, 5, 2419-2432,
521 10.1021/acsearthspacechem.1c00102, 2021.

522 Cui, T., Zeng, Z., dos Santos, E. O., Zhang, Z., Chen, Y., Zhang, Y., Rose, C. A., Budisulistiorini, S. H.,

523 Collins, L. B., Bodnar, W. M., de Souza, R. A. F., Martin, S. T., Machado, C. M. D., Turpin, B. J.,

524 Gold, A., Ault, A. P., and Surratt, J. D.: Development of a hydrophilic interaction liquid

525 chromatography (HILIC) method for the chemical characterization of water-soluble isoprene

526 epoxydiol (IEPOX)-derived secondary organic aerosol, *Environ. Sci.: Process. Impacts*, 20, 1524-

527 1536, 10.1039/c8em00308d, 2018.

528 Darer, A. I., Cole-Filipiak, N. C., O'Connor, A. E., and Elrod, M. J.: Formation and Stability of

529 Atmospherically Relevant Isoprene-Derived Organosulfates and Organonitrates, *Environ. Sci.*

530 *Technol.*, 45, 1895-1902, 10.1021/es103797z, 2011.

531 Ding, S., Chen, Y., Devineni, S. R., Pavuluri, C. M., and Li, X.-D.: Distribution characteristics of

532 organosulfates (OSs) in PM2.5 in Tianjin, Northern China: Quantitative analysis of total and three

533 OS species, *Sci. Total Environ.*, 834, 10.1016/j.scitotenv.2022.155314, 2022.

534 Ding, X., He, Q.-F., Shen, R.-Q., Yu, Q.-Q., and Wang, X.-M.: Spatial distributions of secondary

535 organic aerosols from isoprene, monoterpenes, β -caryophyllene, and aromatics over China during

536 summer, *J. Geophys. Res. Atmos.*, 119, 11,877-811,891, 10.1002/2014jd021748, 2014.

537 Ding, X., He, Q.-F., Shen, R.-Q., Yu, Q.-Q., Zhang, Y.-Q., Xin, J.-Y., Wen, T.-X., and Wang, X.-M.:

538 Spatial and seasonal variations of isoprene secondary organic aerosol in China: Significant impact

539 of biomass burning during winter, *Sci. Rep.*, 6, 10.1038/srep20411, 2016a.

540 Ding, X., Zhang, Y.-Q., He, Q.-F., Yu, Q.-Q., Wang, J.-Q., Shen, R.-Q., Song, W., Wang, Y.-S., and

541 Wang, X.-M.: Significant Increase of Aromatics-Derived Secondary Organic Aerosol during Fall

542 to Winter in China, *Environ. Sci. Technol.*, 51, 7432-7441, 10.1021/acs.est.6b06408, 2017.

543 Ding, X., Zhang, Y. Q., He, Q. F., Yu, Q. Q., Shen, R. Q., Zhang, Y., Zhang, Z., Lyu, S. J., Hu, Q. H.,

544 Wang, Y. S., Li, L. F., Song, W., and Wang, X. M.: Spatial and seasonal variations of secondary

545 organic aerosol from terpenoids over China, J. Geophys. Res. Atmos., 121,
546 10.1002/2016jd025467, 2016b.

547 Duporté, G., Flaud, P. M., Geneste, E., Augagneur, S., Pangui, E., Lamkaddam, H., Gratien, A.,
548 Doussin, J. F., Budzinski, H., Villenave, E., and Perrauidin, E.: Experimental Study of the
549 Formation of Organosulfates from α -Pinene Oxidation. Part I: Product Identification, Formation
550 Mechanisms and Effect of Relative Humidity, J. Phys. Chem. A, 120, 7909-7923,
551 10.1021/acs.jpca.6b08504, 2016.

552 Duporté, G., Flaud, P. M., Kammer, J., Geneste, E., Augagneur, S., Pangui, E., Lamkaddam, H.,
553 Gratien, A., Doussin, J. F., Budzinski, H., Villenave, E., and Perrauidin, E.: Experimental Study of
554 the Formation of Organosulfates from α -Pinene Oxidation. 2. Time Evolution and Effect of
555 Particle Acidity, J. Phys. Chem. A, 124, 409-421, 10.1021/acs.jpca.9b07156, 2019.

556 Fleming, L. T., Ali, N. N., Blair, S. L., Roveretto, M., George, C., and Nizkorodov, S. A.: Formation of
557 Light-Absorbing Organosulfates during Evaporation of Secondary Organic Material Extracts in
558 the Presence of Sulfuric Acid, ACS Earth Space Chem., 3, 947-957,
559 10.1021/acsearthspacechem.9b00036, 2019.

560 Gilardoni, S., Massoli, P., Paglione, M., Giulianelli, L., Carbone, C., Rinaldi, M., Decesari, S.,
561 Sandrini, S., Costabile, F., Gobbi, G. P., Pietrogrande, M. C., Visentin, M., Scotto, F., Fuzzi, S.,
562 and Facchini, M. C.: Direct observation of aqueous secondary organic aerosol from biomass-
563 burning emissions, Proc. Natl. Acad. Sci. U.S.A., 113, 10013-10018, 10.1073/pnas.1602212113,
564 2016.

565 Guenther, A. B., Zimmerman, P. R., Harley, P. C., Monson, R. K., and Fall, R.: Isoprene and
566 monoterpane emission rate variability J. Geophys. Res. Atmos., 98, 12609-12617, 1993.

567 He, L. Y., Lin, Y., Huang, X. F., Guo, S., Xue, L., Su, Q., Hu, M., Luan, S. J., and Zhang, Y. H.:
568 Characterization of high-resolution aerosol mass spectra of primary organic aerosol emissions
569 from Chinese cooking and biomass burning, *Atmos. Chem. Phys.*, 10, 11535-11543, 10.5194/acp-
570 10-11535-2010, 2010.

571 Hettiyadura, A. P. S., Al-Naiema, I. M., Hughes, D. D., Fang, T., and Stone, E. A.: Organosulfates in
572 Atlanta, Georgia: anthropogenic influences on biogenic secondary organic aerosol formation,
573 *Atmos. Chem. Phys.*, 19, 3191-3206, 10.5194/acp-19-3191-2019, 2019.

574 Hettiyadura, A. P. S., Stone, E. A., Kundu, S., Baker, Z., Geddes, E., Richards, K., and Humphry, T.:
575 Determination of atmospheric organosulfates using HILIC chromatography with MS detection,
576 *Atmos. Meas. Tech.*, 8, 2347-2358, 10.5194/amt-8-2347-2015, 2015.

577 Hettiyadura, A. P. S., Jayarathne, T., Baumann, K., Goldstein, A. H., de Gouw, J. A., Koss, A., Keutsch,
578 F. N., Skog, K., and Stone, E. A.: Qualitative and quantitative analysis of atmospheric
579 organosulfates in Centreville, Alabama, *Atmos. Chem. Phys.*, 17, 1343-1359, 10.5194/acp-17-
580 1343-2017, 2017.

581 Huang, L., Wang, Y., Zhao, Y., Hu, H., Yang, Y., Wang, Y., Yu, J. Z., Chen, T., Cheng, Z., Li, C., Li, Z.,
582 and Xiao, H.: Biogenic and Anthropogenic Contributions to Atmospheric Organosulfates in a
583 Typical Megacity in Eastern China, *J. Geophys. Res. Atmos.*, 128, 10.1029/2023jd038848, 2023.

584 Jiang, H., Cai, J., Feng, X., Chen, Y., Wang, L., Jiang, B., Liao, Y., Li, J., Zhang, G., Mu, Y., and Chen,
585 J.: Aqueous-Phase Reactions of Anthropogenic Emissions Lead to the High Chemodiversity of
586 Atmospheric Nitrogen-Containing Compounds during the Haze Event, *Environ. Sci. Technol.*, 57,
587 16500-16511, 10.1021/acs.est.3c06648, 2023.

588 Kanellopoulos, P. G., Kotsaki, S. P., Chrysochou, E., Koukoulakis, K., Zacharopoulos, N.,

589 Philippopoulos, A., and Bakeas, E.: PM2.5-bound organosulfates in two Eastern Mediterranean
590 cities: The dominance of isoprene organosulfates, *Chemosphere*, 297,
591 10.1016/j.chemosphere.2022.134103, 2022.

592 Kristensen, K., Bilde, M., Aalto, P. P., Petäjä, T., and Glasius, M.: Denuder/filter sampling of organic
593 acids and organosulfates at urban and boreal forest sites: Gas/particle distribution and possible
594 sampling artifacts, *Atmos. Environ.*, 130, 36-53, 10.1016/j.atmosenv.2015.10.046, 2016.

595 Li, J., Wang, G., Wu, C., Cao, C., Ren, Y., Wang, J., Li, J., Cao, J., Zeng, L., and Zhu, T.:
596 Characterization of isoprene-derived secondary organic aerosols at a rural site in North China
597 Plain with implications for anthropogenic pollution effects, *Sci. Rep.*, 8, 10.1038/s41598-017-
598 18983-7, 2018.

599 Li, L., Yang, W., Xie, S., and Wu, Y.: Estimations and uncertainty of biogenic volatile organic
600 compound emission inventory in China for 2008–2018, *Sci. Total Environ.*, 733,
601 10.1016/j.scitotenv.2020.139301, 2020.

602 Li, L. Y. and Xie, S. D.: Historical variations of biogenic volatile organic compound emission
603 inventories in China, 1981–2003, *Atmos. Environ.*, 95, 185-196, 10.1016/j.atmosenv.2014.06.033,
604 2014.

605 Lin, X., Xu, Y., Zhu, R. G., Xiao, H. W., and Xiao, H. Y.: Proteinaceous Matter in PM2.5 in Suburban
606 Guiyang, Southwestern China: Decreased Importance in Long-Range Transport and Atmospheric
607 Degradation, *J. Geophys. Res. Atmos.*, 128, 10.1029/2023jd038516, 2023.

608 Liu, T., Xu, Y., Sun, Q. B., Xiao, H. W., Zhu, R. G., Li, C. X., Li, Z. Y., Zhang, K. Q., Sun, C. X., and
609 Xiao, H. Y.: Characteristics, Origins, and Atmospheric Processes of Amines in Fine Aerosol
610 Particles in Winter in China, *J. Geophys. Res. Atmos.*, 128, 10.1029/2023jd038974, 2023.

611 Luk'acs, H., Gelencs'er, A., Hoffer, A., Kiss, G., Horv'ath, K., and Harty'ani, Z.: Quantitative
612 assessment of organosulfates in size-segregated rural fine aerosol, *Atmos. Chem. Phys.*, 9, 231-
613 238, 10.5194/acp-9-231-2009, 2009.

614 Ma, Q., Cai, S., Wang, S., Zhao, B., Martin, R. V., Brauer, M., Cohen, A., Jiang, J., Zhou, W., Hao, J.,
615 Frostad, J., Forouzanfar, M. H., and Burnett, R. T.: Impacts of coal burning on ambient PM2.5
616 pollution in China, *Atmos. Chem. Phys.*, 17, 4477-4491, 10.5194/acp-17-4477-2017, 2017.

617 Mason, S. A., Field, R. J., Yokelson, R. J., Kochivar, M. A., Tinsley, M. R., Ward, D. E., and Hao, W.
618 M.: Complex effects arising in smoke plume simulations due to inclusion of direct emissions of
619 oxygenated organic species from biomass combustion, *J. Geophys. Res. Atmos.*, 106, 12527-
620 12539, 10.1029/2001jd900003, 2001.

621 Nozière, B., Ekström, S., Alsberg, T., and Holmström, S.: Radical-initiated formation of organosulfates
622 and surfactants in atmospheric aerosols, *Geophys. Res. Lett.*, 37, n/a-n/a, 10.1029/2009gl041683,
623 2010.

624 Riva, M., Tomaz, S., Cui, T., Lin, Y.-H., Perraudin, E., Gold, A., Stone, E. A., Villenave, E., and
625 Surratt, J. D.: Evidence for an Unrecognized Secondary Anthropogenic Source of Organosulfates
626 and Sulfonates: Gas-Phase Oxidation of Polycyclic Aromatic Hydrocarbons in the Presence of
627 Sulfate Aerosol, *Environ. Sci. Technol.*, 49, 6654-6664, 10.1021/acs.est.5b00836, 2015.

628 Riva, M., Chen, Y., Zhang, Y., Lei, Z., Olson, N. E., Boyer, H. C., Narayan, S., Yee, L. D., Green, H. S.,
629 Cui, T., Zhang, Z., Baumann, K., Fort, M., Edgerton, E., Budisulistiorini, S. H., Rose, C. A.,
630 Ribeiro, I. O., e Oliveira, R. L., dos Santos, E. O., Machado, C. M. D., Szopa, S., Zhao, Y., Alves,
631 E. G., de Sá, S. S., Hu, W., Knipping, E. M., Shaw, S. L., Duvoisin Junior, S., de Souza, R. A. F.,
632 Palm, B. B., Jimenez, J.-L., Glasius, M., Goldstein, A. H., Pye, H. O. T., Gold, A., Turpin, B. J.,

633 Vizuete, W., Martin, S. T., Thornton, J. A., Dutcher, C. S., Ault, A. P., and Surratt, J. D.: Increasing
634 Isoprene Epoxydiol-to-Inorganic Sulfate Aerosol Ratio Results in Extensive Conversion of
635 Inorganic Sulfate to Organosulfur Forms: Implications for Aerosol Physicochemical Properties,
636 Environ. Sci. Technol., 53, 8682-8694, 10.1021/acs.est.9b01019, 2019.

637 Schindelka, J., Iinuma, Y., Hoffmann, D., and Herrmann, H.: Sulfate radical-initiated formation of
638 isoprene-derived organosulfates in atmospheric aerosols, Faraday Discuss., 165,
639 10.1039/c3fd00042g, 2013.

640 Simpson, I. J., Akagi, S. K., Barletta, B., Blake, N. J., Choi, Y., Diskin, G. S., Fried, A., Fuelberg, H. E.,
641 Meinardi, S., Rowland, F. S., Vay, S. A., Weinheimer, A. J., Wennberg, P. O., Wiebring, P.,
642 Wisthaler, A., Yang, M., Yokelson, R. J., and Blake, D. R.: Boreal forest fire emissions in fresh
643 Canadian smoke plumes: C₁-C₁₀ volatile organic compounds (VOCs), CO₂, CO, NO₂, NO, HCN
644 and CH₃CN, Atmos. Chem. Phys., 11, 6445-6463, 10.5194/acp-11-6445-2011, 2011.

645 Song, J., Li, M., Jiang, B., Wei, S., Fan, X., and Peng, P. a.: Molecular Characterization of Water-
646 Soluble Humic like Substances in Smoke Particles Emitted from Combustion of Biomass
647 Materials and Coal Using Ultrahigh-Resolution Electrospray Ionization Fourier Transform Ion
648 Cyclotron Resonance Mass Spectrometry, Environ. Sci. Technol., 52, 2575-2585,
649 10.1021/acs.est.7b06126, 2018.

650 Song, J., Li, M., Fan, X., Zou, C., Zhu, M., Jiang, B., Yu, Z., Jia, W., Liao, Y., and Peng, P. a.:
651 Molecular Characterization of Water- and Methanol-Soluble Organic Compounds Emitted from
652 Residential Coal Combustion Using Ultrahigh-Resolution Electrospray Ionization Fourier
653 Transform Ion Cyclotron Resonance Mass Spectrometry, Environ. Sci. Technol., 53, 13607-
654 13617, 10.1021/acs.est.9b04331, 2019.

655 Surratt, J. D., Kroll, J. H., Kleindienst, T. E., Edney, E. O., Claeys, M., Sorooshian, A., Ng, L.,

656 Offenberg, J. H., Lewandowski, M., Jaoui, M., Flagan, R. C., and Seinfeld, J. H.: Evidence for

657 organosulfates in secondary organic aerosol., Environ. Sci. Technol., 41, 517-527, 2007.

658 Surratt, J. D., Gómez-González, Y., Chan, A. W., Vermeylen, R., Shahgholi, M., Kleindienst, T. E.,

659 Edney, E. O., Offenberg, J. H., Lewandowski, M., Jaoui, M., Maenhaut, M. W., Claeys, M.,

660 Flagan, R. C., and Seinfeld, J. H.: Organosulfate Formation in Biogenic Secondary Organic

661 Aerosol, J. Phys. Chem. A, 112, 8345-8378, 2008.

662 Tang, J., Li, J., Su, T., Han, Y., Mo, Y., Jiang, H., Cui, M., Jiang, B., Chen, Y., Tang, J., Song, J., Peng,

663 P. a., and Zhang, G.: Molecular compositions and optical properties of dissolved brown carbon in

664 biomass burning, coal combustion, and vehicle emission aerosols illuminated by excitation–

665 emission matrix spectroscopy and Fourier transform ion cyclotron resonance mass spectrometry

666 analysis, Atmos. Chem. Phys., 20, 2513-2532, 10.5194/acp-20-2513-2020, 2020.

667 Tao, S., Lu, X., Levac, N., Bateman, A. P., Nguyen, T. B., Bones, D. L., Nizkorodov, S. A., Laskin, J.,

668 Laskin, A., and Yang, X.: Molecular Characterization of Organosulfates in Organic Aerosols from

669 Shanghai and Los Angeles Urban Areas by Nanospray-Desorption Electrospray Ionization High-

670 Resolution Mass Spectrometry, Environ. Sci. Technol., 48, 10993-11001, 10.1021/es5024674,

671 2014.

672 Wach, P., Spólnik, G., Rudziński, K. J., Skotak, K., Claeys, M., Danikiewicz, W., and Szmigielski, R.:

673 Radical oxidation of methyl vinyl ketone and methacrolein in aqueous droplets: Characterization

674 of organosulfates and atmospheric implications, Chemosphere, 214, 1-9,

675 10.1016/j.chemosphere.2018.09.026, 2019.

676 Wang, K., Zhang, Y., Huang, R.-J., Wang, M., Ni, H., Kampf, C. J., Cheng, Y., Bilde, M., Glasius, M.,

677 and Hoffmann, T.: Molecular Characterization and Source Identification of Atmospheric
678 Particulate Organosulfates Using Ultrahigh Resolution Mass Spectrometry, *Environ. Sci. Technol.*,
679 53, 6192-6202, 10.1021/acs.est.9b02628, 2019.

680 Wang, Y., Ma, Y., Kuang, B., Lin, P., Liang, Y., Huang, C., and Yu, J. Z.: Abundance of organosulfates
681 derived from biogenic volatile organic compounds: Seasonal and spatial contrasts at four sites in
682 China, *Sci. Total Environ.*, 806, 10.1016/j.scitotenv.2021.151275, 2022.

683 Wang, Y., Zhao, Y., Wang, Y., Yu, J.-Z., Shao, J., Liu, P., Zhu, W., Cheng, Z., Li, Z., Yan, N., and Xiao,
684 H.: Organosulfates in atmospheric aerosols in Shanghai, China: seasonal and interannual
685 variability, origin, and formation mechanisms, *Atmos. Chem. Phys.*, 21, 2959-2980, 10.5194/acp-
686 21-2959-2021, 2021.

687 Wang, Y., Hu, M., Wang, Y.-C., Li, X., Fang, X., Tang, R., Lu, S., Wu, Y., Guo, S., Wu, Z., Hallquist,
688 M., and Yu, J. Z.: Comparative Study of Particulate Organosulfates in Contrasting Atmospheric
689 Environments: Field Evidence for the Significant Influence of Anthropogenic Sulfate and NO_x,
690 *Environ. Sci. Technol. Lett.*, 7, 787-794, 10.1021/acs.estlett.0c00550, 2020.

691 Wang, Y., Hu, M., Lin, P., Guo, Q., Wu, Z., Li, M., Zeng, L., Song, Y., Zeng, L., Wu, Y., Guo, S.,
692 Huang, X., and He, L.: Molecular Characterization of Nitrogen-Containing Organic Compounds
693 in Humic-like Substances Emitted from Straw Residue Burning, *Environ. Sci. Technol.*, 51, 5951-
694 5961, 10.1021/acs.est.7b00248, 2017.

695 Wang, Y., Zhang, Y., Li, W., Wu, G., Qi, Y., Li, S., Zhu, W., Yu, J. Z., Yu, X., Zhang, H.-H., Sun, J.,
696 Wang, W., Sheng, L., Yao, X., Gao, H., Huang, C., Ma, Y., and Zhou, Y.: Important Roles and
697 Formation of Atmospheric Organosulfates in Marine Organic Aerosols: Influence of
698 Phytoplankton Emissions and Anthropogenic Pollutants, *Environ. Sci. Technol.*, 57, 10284-10294,

699 10.1021/acs.est.3c01422, 2023.

700 Wang, Y., Hu, M., Guo, S., Wang, Y., Zheng, J., Yang, Y., Zhu, W., Tang, R., Li, X., Liu, Y., Le Breton,
701 M., Du, Z., Shang, D., Wu, Y., Wu, Z., Song, Y., Lou, S., Hallquist, M., and Yu, J.: The secondary
702 formation of organosulfates under interactions between biogenic emissions and anthropogenic
703 pollutants in summer in Beijing, *Atmos. Chem. Phys.*, 18, 10693-10713, 10.5194/acp-18-10693-
704 2018, 2018.

705 Xu, J., Shen, G., Fu, B., Han, Y., Suo, X., Chen, Z., Lai, Y., Li, J., Li, L., Han, L., Tao, S., and Li, B.:
706 Emissions of Particulate and Previously Ignored Gaseous Phosphorus from Coal and Biomass
707 Combustion in Household Stoves, *Environ. Sci. Technol. Lett.*, 10, 1011-1016,
708 10.1021/acs.estlett.3c00029, 2023a.

709 Xu, Y., Dong, X. N., Xiao, H. Y., Zhou, J. X., and Wu, D. S.: Proteinaceous Matter and Liquid Water in
710 Fine Aerosols in Nanchang, Eastern China: Seasonal Variations, Sources, and Potential
711 Connections, *J. Geophys. Res. Atmos.*, 127, 10.1029/2022jd036589, 2022.

712 Xu, Y., Dong, X.-N., He, C., Wu, D.-S., Xiao, H.-W., and Xiao, H.-Y.: Mist cannon trucks can
713 exacerbate the formation of water-soluble organic aerosol and PM_{2.5} pollution in the road
714 environment, *Atmos. Chem. Phys.*, 23, 6775-6788, 10.5194/acp-23-6775-2023, 2023b.

715 Xu, Y., Lin, X., Sun, Q. B., Xiao, H. W., Xiao, H., and Xiao, H. Y.: Elaborating the Atmospheric
716 Transformation of Combined and Free Amino Acids From the Perspective of Observational
717 Studies, *J. Geophys. Res. Atmos.*, 129, 10.1029/2024jd040730, 2024a.

718 Xu, Y., Liu, T., Ma, Y.-J., Sun, Q.-B., Xiao, H.-W., Xiao, H., Xiao, H.-Y., and Liu, C.-Q.: Measurement
719 report: Occurrence of aminiums in PM2.5 during winter in China – aminium outbreak during
720 polluted episodes and potential constraints, *Atmos. Chem. Phys.*, 24, 10531-10542, 10.5194/acp-

721 24-10531-2024, 2024b.

722 Xu, Y., Miyazaki, Y., Tachibana, E., Sato, K., Ramasamy, S., Mochizuki, T., Sadanaga, Y., Nakashima,
723 Y., Sakamoto, Y., Matsuda, K., and Kajii, Y.: Aerosol Liquid Water Promotes the Formation of
724 Water-Soluble Organic Nitrogen in Submicrometer Aerosols in a Suburban Forest, *Environ. Sci.
725 Technol.*, 54, 1406-1414, 10.1021/acs.est.9b05849, 2020.

726 Yang, T., Xu, Y., Ma, Y.-J., Wang, Y.-C., Yu, J. Z., Sun, Q.-B., Xiao, H.-W., Xiao, H.-Y., and Liu, C.-Q.:
727 Field Evidence for Constraints of Nearly Dry and Weakly Acidic Aerosol Conditions on the
728 Formation of Organosulfates, *Environ. Sci. Technol. Lett.*, 10.1021/acs.estlett.4c00522, 2024.

729 Yang, T., Xu, Y., Ye, Q., Ma, Y.-J., Wang, Y.-C., Yu, J.-Z., Duan, Y.-S., Li, C.-X., Xiao, H.-W., Li, Z.-Y.,
730 Zhao, Y., and Xiao, H.-Y.: Spatial and diurnal variations of aerosol organosulfates in summertime
731 Shanghai, China: potential influence of photochemical processes and anthropogenic sulfate
732 pollution, *Atmos. Chem. Phys.*, 23, 13433-13450, 10.5194/acp-23-13433-2023, 2023.

733 Yang, Y. R., Liu, X. G., Qu, Y., An, J. L., Jiang, R., Zhang, Y. H., Sun, Y. L., Wu, Z. J., Zhang, F., Xu,
734 W. Q., and Ma, Q. X.: Characteristics and formation mechanism of continuous hazes in China: a
735 case study during the autumn of 2014 in the North China Plain, *Atmos. Chem. Phys.*, 15, 8165-
736 8178, 10.5194/acp-15-8165-2015, 2015.

737 Yu, Q., Ding, X., He, Q., Yang, W., Zhu, M., Li, S., Zhang, R., Shen, R., Zhang, Y., Bi, X., Wang, Y.,
738 Peng, P. a., and Wang, X.: Nationwide increase of polycyclic aromatic hydrocarbons in ultrafine
739 particles during winter over China revealed by size-segregated measurements, *Atmos. Chem.
740 Phys.*, 20, 14581-14595, 10.5194/acp-20-14581-2020, 2020.

741 Zhang, L., Li, J., Li , Y., Liu, X., ;, Luo, Z., Shen, G., and Tao, S.: Comparison of water-soluble and
742 water-insoluble organic compositions attributing to different light absorption efficiency between

743 residential coal and biomass burning emissions *Atmos. Chem. Phys.*, 24, 6323-6337, 10.5194/acp-
744 24-6323-2024, 2024.

745 Zhang, L., Hu, B., Liu, X., Luo, Z., Xing, R., Li, Y., Xiong, R., Li, G., Cheng, H., Lu, Q., Shen, G., and
746 Tao, S.: Variabilities in Primary N-Containing Aromatic Compound Emissions from Residential
747 Solid Fuel Combustion and Implications for Source Tracers, *Environ. Sci. Technol.*, 56, 13622-
748 13633, 10.1021/acs.est.2c03000, 2022.

749 Zhang, Y., Zhang, R., Yu, J., Zhang, Z., Yang, W., Zhang, H., Lyu, S., Wang, Y., Dai, W., Wang, Y., and
750 Wang, X.: Isoprene Mixing Ratios Measured at Twenty Sites in China During 2012–2014:
751 Comparison With Model Simulation, *J. Geophys. Res. Atmos.*, 125, 10.1029/2020jd033523, 2020.

752 Zhou, Y., Xing, X., Lang, J., Chen, D., Cheng, S., Wei, L., Wei, X., and Liu, C.: A comprehensive
753 biomass burning emission inventory with high spatial and temporal resolution in China, *Atmos.*
754 *Chem. Phys.*, 17, 2839-2864, 10.5194/acp-17-2839-2017, 2017.

755 Zhu, Y., Yang, L., Chen, J., Wang, X., Xue, L., Sui, X., Wen, L., Xu, C., Yao, L., Zhang, J., Shao, M.,
756 Lu, S., and Wang, W.: Characteristics of ambient volatile organic compounds and the influence of
757 biomass burning at a rural site in Northern China during summer 2013, *Atmos. Environ.*, 124,
758 156-165, 10.1016/j.atmosenv.2015.08.097, 2016.

759